International Journal of Thermal Sciences 49 (2010) 471–478

Contents lists available at ScienceDirect

International Journal of Thermal Sciences

journal homepage: www.elsevier.com/locate/ijts

Prediction of nanofluid convective heat transfer using the dispersion model

A. Mokmeli, M. Saffar-Avval*

Energy and Control Center of Excellence, Department of Mechanical Engineering, Amirkabir University of Technology (Tehran Polytechnic), Hafez Avenue, P.O. Box 15875-4413, Tehran, Iran

ARTICLE INFO

Article history:
Received 2 September 2008
Received in revised form
14 September 2009
Accepted 14 September 2009
Available online 23 October 2009

Keywords:
Nanofluids
Convective heat transfer
Laminar flow
Dispersion model
Nanoparticle size

ABSTRACT

The laminar convective heat transfer behavior of nanofluids through a straight tube is numerically investigated in this paper. A new mechanism which is proposed to explain considerable enhancement of nanofluids heat transfer is dispersion that intends to consider the irregular movements of the nanoparticles. Applying this additional mechanism leads to promising results in comparison with the predictions by traditional homogenous model with effective properties. To validate the dispersion model results, the experimental results for three kinds of nanofluids are used. Also the effect of nanoparticle size on nanofluid heat transfer is examined. The obtained results show good agreement between the theoretical and experimental results.

1. Introduction

The performance of the conventional Heat transfer fluids such as water, minerals oil and ethylene glycol is often limited by their low thermal properties which are the main limitations for industrial process intensification and device miniaturization. Adding high conductivity solid particles to a fluid is one of the known heat transfer enhancement methods. If a suspension of millimeter or micrometer sized particles is used, although showing some enhancement, experienced problems such as poor suspension stability, rapid sedimentation, channel clogging, corrosion, pipeline erosion and great pressure drop which are particularly serious for system performance are accrued. Because of these disadvantages, this method for heat transfer enhancement was not vastly used [1]. To prevent the above disadvantages, the use of nanometer particles was proposed. This new kind of fluids named "Nanofluids" was introduced in 1995 [2]. The term nanofluid is used to describe a solid-liquid mixture which consists of a base liquid with dilute volume fraction of high conductivity solid nanoparticles. The nanofluids have a unique feature which is quite different from those of the conventional solid–liquid mixtures in which millimeter or micrometer sized particles are added [3]. Compared with suspended particles of millimeter or micrometer dimensions, nanofluids show better stability and rheological properties, reported higher thermal conductivities, and no penalty in pressure drop. Because of the excellent potential of nanofluids in heat transfer enhancement, it is expected that the nanofluid will become the next generation of heat transfer fluid for thermal engineering [4].

Nanoparticles can be produced from several processes such as gas condensation, mechanical attrition or chemical precipitation techniques. The preparation of a nanofluid begins by direct mixing of the base fluid with Nanoparticles. Then some methods used for stabilizing the suspensions: 1 – adjusting the pH value of suspensions; 2 – using surface activators or dispersants; 3 – using ultrasonic vibration. These methods can change the surface properties of the suspended particles and can be used to suppress the formation of particle clusters in order to obtain stable suspensions. The use of these techniques depends on the required application of the nanofluid. Selection of suitable activators and dispersants depends mainly upon the properties of the solutions and particles [5,6].

The enhancement of the local heat transfer coefficient is much more dramatic than the enhancement of the available theoretical predictions. Different reasons such as increasing the nanoparticles surface area compared with micron-sized particles [6], particle migration [1], intensification of turbulence or eddies [4], dispersion of the suspended nanoparticles have been suggested [4,6], all of them leading to suppression or interruption of the boundary layer.

There are two different approaches to investigate the enhanced heat transfer of the suspensions: the two-phase one and the single-phase one. The first provides the possibility of understanding the functions of both the fluid phase and the solid particle in the heat transfer process, but needs much computation time and computer

* Corresponding author. Tel.: +98 21 66405844; fax: +98 21 66419736.
E-mail address: mavval@aut.ac.ir (M. Saffar-Avval).

1290-0729/$ – see front matter © 2009 Elsevier Masson SAS. All rights reserved.
doi:10.1016/j.ijthermalsci.2009.09.005

Nomenclature

C	dispersion coefficient
C_p	specific heat (J kg^{-1} K^{-1})
d	nanoparticle diameter (m)
f	Fanning friction factor
h	local heat transfer coefficient (W m^{-2} K^{-1})
k	thermal conductivity (W m^{-1} K^{-1})
L	length dimensional symbol
M	mass dimensional symbol
n	shape factor
Nu	Nusselt number
P	pressure (Pa)
Pe	Peclet number
Pr	Prandtl number
q''	wall heat flux (w m^{-2})
r	radial coordinate
R	inner radius of the tube (m)
Re	Reynolds number
t	time (s)
T	temperature (K) and time dimensional symbol
u	velocity (m s^{-1})
v	preliminary velocity (m s^{-1})
V	volume (m^3)
x	distance along the tube (m) or axial coordinate

Greek symbols

α	thermal diffusivity (m^2 s^{-1})
ϕ	volume fraction of the nanoparticles
μ	dynamic viscosity (kg m^{-1} s^{-1})
ν	kinematic viscosity (m^2 s^{-1})
ρ	density (kg m^{-3})
ε	porosity coefficient
θ	azimuthal coordinate
Θ	temperature dimensional symbol

Subscripts

d	dispersion effect
f	fluid
in	tube inlet
nf	nanofluid
p	particle
r	radial direction
s	solid
x	axial direction

Superscripts

$\rightarrow$	vector
$-$	average
$'$	fluctuation
$*$	dimensionless variable

capacity [6]. By combining Lagrangian statistics and DNS (direct numerical simulation) Sato et al. (1998) applied this approach to analyze the mechanism of two-phase heat and turbulent transport by solid particles (on the micrometer order) suspended in a gas flow [7].

Another two-phase model is mixture model. The mixture model, based on a single fluid two phase approach assumes that the coupling between phases is strong, and particles closely follow the flow. The two phases are assumed to be interpenetrating, meaning that each phase has its own velocity vector field and slip velocity (relative velocity) is defined as the velocity of the nanoparticle phase relative to the velocity of the base fluid phase. Within any control volume there is a volume fraction of primary phase and also a volume fraction of the secondary phase. This model is employed by Behzadmehr et al. (2007) in the simulation of nanofluids [8]. This model prediction is more consistent with the experimental results.

The second approach assumes that both the fluid phase and particles are in a thermal equilibrium condition and flow at the same velocity. This approach which is based on the single phase flow is simpler and takes less computation time. In cases that the main interest is focused on heat transfer calculations, this approach may be more suitable [6].

Homogenous model is one of the nanofluid single phase models. This model differs from conventional pure fluid model only in the effective properties. It means that the continuity, Navier–Stokes and the energy equations are used with the nanofluid effective properties. According to this model, usual correlations of flow and heat transfer feature of a single phase fluid can be generalized to the nanofluid. Maiga et Al (2005) studied nanofluid based on this model [9]; this model is not competent to predict the heat transfer features of nanofluids [4,10]. Another single phase model uses one more heat transfer mechanism to the common ones, this model is called dispersion model. The present study aims to drive the mathematical model of the dispersion mechanism, and shows that this model has the ability to predict the nanofluid heat transfer more accurately.

2. Nanofluid properties

The Nanofluid transport and thermal properties are quite different from the base fluid. Effective density and thermal capacity of nanofluids are calculated using some classical formulas as well known for two phase fluids accurately [9].

$$\rho_{nf} = (1-\phi)\rho_f + \phi\rho_p \tag{1}$$

$$(\rho C_p)_{nf} = (1-\phi)(\rho C_p)_f + \phi(\rho C_p)_p \tag{2}$$

The viscosity of the nanofluids can be estimated with the existing correlations for the two phase mixture [3]. For example, the well known Einstein's formula for evaluating the effective viscosity of a dilute suspension of small rigid spherical particles can be employed [11].

$$\mu_{nf} = \mu_f(1+2.5\phi) \tag{3}$$

There are some theoretical models for thermal conductivity of the solid-liquid mixtures with relatively large particles of the order of micrometers or millimeters. For example Hamilton and Crosser (1962) developed the following model for solid–liquid mixtures in which the ratio of conductivity of two phases is larger than 100 [12]:

$$\frac{k_{nf}}{k_f} = \frac{k_p + (n-1)k_f - (n-1)\phi(k_f - k_p)}{k_p + (n-1)k_f + \phi(k_f - k_p)} \tag{4}$$

But the results from all of the available experimental studies indicate that nanofluids have substantially higher thermal conductivity than those predicted by existing models for the mixtures, therefore the application of these models like equation (4) to the nanofluids is not always permitted [13]. The nanofluid thermal conductivity is significantly enhanced, for example the thermal conductivity enhancement of the nanofluid containing Cu

nanoparticles in ethylene glycol has reported almost 40% in Eastman et al. research [14].

The conventional approach of the effective thermal conductivity of mixtures derived from continuum level phenomenological formulations that assume diffusive heat transport in both liquid and solid phases. This assumption is not sufficient for nanofluids. Some other potential mechanisms of enhanced conduction in nanofluids are introduced by researchers and according to each one they have developed various models and formulas. Nanoparticles Brownian motion [15], liquid layering at particle interface [16–19], nanoparticles clustering and aggregation, nanoparticles ballistic motion, nanoparticles migration [20] are some examples of new suggested mechanisms [13]. But no one is generally accepted and responsible for all cases. Nowadays the only reliable method for revealing nanofluid thermal properties is the experiment. In present study, the experimental results for nanofluid thermal properties have been adopted.

3. Dispersion model

The dispersion is a known theory in the porous media subject. Consider saturated flow through a porous medium, and let a portion of the flow domain contain a certain mass of solute. This solute will be referred as a tracer, the tracer which is a labeled portion of the same liquid, may be identified by its density, color, electrical conductivity, etc. Experience shows that as flow takes place the tracer gradually spreads and occupies an ever increasing portion of the flow domain, beyond the region it is expected to occupy according to the average flow alone. This spreading phenomenon is called hydrodynamic dispersion in a porous medium. Because of the velocity distribution within each pore, variations in local velocity, both in magnitude and direction, occur. In addition, the interaction between the solid surface of the porous matrix and the liquid cause changes in the concentration of the tracer in the flowing liquid. Variations in local velocity and changes in the concentration cause any initial tracer mass within the flow domain to spread and occupy an ever increasing volume of the porous medium [21]. Considering simultaneous fluid flow and heat transfer in porous media, the role of the macroscopic (Darcean) and microscopic (pore level) velocity field on the temperature field needs to be examined. Influence of the effect of the pore level velocity non uniformity on the temperature distribution is called thermal dispersion effect [22].

For mathematical modeling of dispersion phenomena in the porous media, assume that irregular movements of the ultra fine particles induce small perturbations of both the temperature and velocity of the nanofluid, i.e., $T'$and $\overrightarrow{u'}$, respectively. Thus, the intrinsic phase averages are given as [3]:

$$T = \overline{T} + T' \tag{5}$$

$$\overrightarrow{u} = \overline{\overrightarrow{u}} + \overrightarrow{u'} \tag{6}$$

Where

$$\overline{T} = \frac{1}{V_f}\int_{V_f} T\mathrm{d}V_f \tag{7}$$

$$\overline{\overrightarrow{u}} = \frac{1}{V_f}\int_{V_f} \overrightarrow{u}\, dV_f \tag{8}$$

It is evident that the volumetric average of the temperature fluctuation is zero.

$$\frac{1}{V_f}\int_{V_f} T'\mathrm{d}V_f = 0 \tag{9}$$

In the light of the procedure described by Kaviany [22] and by assuming that the boundary surface between the fluid and the particles is so small that can be neglected, one obtains the following expression for the energy equation:

$$\frac{\partial \overline{T}}{\partial t} + \overline{\overrightarrow{u}}\cdot\nabla\overline{T} = \nabla\cdot\alpha_f\nabla\overline{T} - \nabla(\overline{u'T'}) \tag{10}$$

The second term in right hand of equation (10) indicates the effect of thermal dispersion. By means of an analogy with the treatment of turbulence, this term can be expressed as:

$$\overline{u'T'} = -k_\mathrm{d}\cdot\nabla\overline{T} \tag{11}$$

Where k_d is the dispersed thermal conductivity. Thermal dispersion diffusivity (α_d) in porous media is dependent upon the below factors [22]:

$$\frac{\alpha_\mathrm{d}}{\alpha_\mathrm{f}} = \text{function}\left(\mathrm{Re}, \mathrm{Pr}, \varepsilon, \text{structure}, \frac{k_\mathrm{s}}{k_\mathrm{f}}, \frac{(\rho C_\mathrm{p})_s}{(\rho C_\mathrm{p})_f}\right) \tag{12}$$

There are various experimental and theoretical formulas for the dispersion thermal diffusivity in porous media. For example, Baron (1952) introduced a correlation for radial dispersion diffusivity in a disordered porous media as $(1/(5\sim15))\mathrm{Pe}$ [23].

In nanofluid subject, the dispersion considers the effect of chaotic movement of the nanoparticles in the flow and is modeled similar to the method used in porous media. This model was suggested by Xuan and Roetzel (2000) [3]. They have assumed the relations 13 and 14 for representing the dispersed thermal conductivity of the nanofluid [3].

$$k_\mathrm{d} = C(\rho C_\mathrm{p})_{nf} uR \tag{13}$$

$$k_d = C(\rho C_\mathrm{p})_{nf} uRd_p\phi \tag{14}$$

Relation (13) is seems to be incomplete because it does not contain the main parameters of nanofluid namely volume fraction and nanoparticle size. Relation (14) is not plausible because its two sides are not dimensionally compatible; left hand side dimension is $ML^2T^{-3}\Theta^{-1}$ but $MLT^{-3}\Theta^{-1}$ at the other side. Another dispersion model is presented by Xuan and Li who used the Beckman formulas for the axial dispersion coefficient [6].

$$\frac{\alpha_{d,x}}{\alpha_f} = 10.1Ru_x\sqrt{f/2} + 5.03Ru_x \tag{15}$$

In this work, they have assumed the constant axial velocity in the tube cross section that is a misleading simplification. In this case the dispersion thermal diffusivity becomes a constant value and can be added to the thermal diffusivity and represents the effective thermal diffusivity. So they have applied the homogenous model to predict the nanofluid heat transfer, not applying the dispersion model.

As Xuan and Roetzel had suggested the axial dispersed thermal conductivity is ignored [3]. In this research, a correlation for the dispersed thermal conductivity in radial direction is introduced as below:

$$k_d = C(\rho c_p)_{nf}\frac{R\phi}{d_p}\left(\frac{\partial u_x}{\partial r}\right)$$

$$\alpha_d = \frac{k_d}{(\rho c_p)_{nf}} = C\frac{R\phi}{d_p}\left(\frac{\partial u_x}{\partial r}\right) \tag{16}$$

This correlation contains the functional factors of nanofluid heat transfer and can be simplified in the form of Baron correlation for dispersion diffusivity in a disordered porous media. The heat flux can be calculated by using correlation (17):

$$q'' = -\left(k_{nf}\frac{\partial T}{\partial r} + k_d\frac{\partial T}{\partial r}\right)_{r=R} \tag{17}$$

4. Numerical simulation

For the particular applications under consideration, it is assumed that the nanofluids are continuous, Newtonian and incompressible with constant physical properties. Both the compression work and viscous dissipation are assumed negligible in the energy equation, thermal conductivity is explained by Fourier law. Also, nanoparticles are in thermal equilibrium with the base fluid and there is not any body force and heat source in the problem.

The dispersion model approach has been adopted in order to be able to study the thermal behaviors of nanofluids, the energy equation is written as follows:

$$\frac{\partial T}{\partial t} + \frac{1}{r}\frac{\partial}{\partial r}(ru_rT) + \frac{\partial}{\partial x}(u_xT) = \frac{1}{r}\frac{\partial}{\partial r}\left\{(\alpha_{nf}+\alpha_d)r\frac{\partial T}{\partial r}\right\} + \frac{\partial^2 T}{\partial x^2} \tag{18}$$

Dimensionless variables are defined as follows:

$$x^* = \frac{x}{R},\ r^* = \frac{r}{R}\ u_x{}^* = \frac{u_x}{u_{\text{in}}},\ u_r{}^* = \frac{u_r}{u_{\text{in}}}\ t^* = \frac{u_{\text{in}}t}{R},\ p^* = \frac{p}{\rho u_{\text{in}}^2}$$

$$\text{Re} = \frac{2\rho u_{in}R}{\mu}\ \text{Pr} = \frac{\nu}{\alpha}\ Nu = \frac{2hR}{k}$$

$$T^* = \frac{T_{r^*=1} - T}{T_{r^*=1} - T_{\text{in}}}\ \text{uniform wall temperature}$$

$$T^* = \frac{k(T_{\text{in}} - T)}{2q''R}\ \text{uniform wall heat flux} \tag{19}$$

Where u_{in} is the uniform axial velocity at the tube inlet. Under such conditions, the general conservation equations could be written in the dimensionless conservative form in cylindrical coordinate as follows:

$$\frac{1}{r^*}\frac{\partial}{\partial r^*}(r^*u_r^*) + \frac{\partial u_x^*}{\partial x^*} = 0 \tag{20}$$

$$\frac{\partial u_x^*}{\partial t^*} + \frac{1}{r^*}\frac{\partial}{\partial r^*}(r^*u_x^*u_r^*) + \frac{\partial}{\partial x^*}(u_x^{*2}) + \frac{\partial p^*}{\partial x^*} = \frac{2}{\text{Re}}\left[\frac{1}{r^*}\frac{\partial}{\partial r^*}\left(r^*\frac{\partial u_x^*}{\partial r^*}\right) + \frac{\partial^2 u_x^*}{\partial x^{*2}}\right] \tag{21}$$

$$\frac{\partial u_r^*}{\partial t^*} + \frac{1}{r^*}\frac{\partial}{\partial r^*}(r^*u_r^{*2}) + \frac{\partial}{\partial x^*}(u_x^*u_r^*) + \frac{\partial p^*}{\partial r^*} = \frac{2}{\text{Re}}\left[\frac{1}{r^*}\frac{\partial}{\partial r^*}\left(r^*\frac{\partial u_r^*}{\partial r^*}\right) + \frac{\partial}{\partial r^*}\left(\frac{1}{r^*}\frac{\partial}{\partial r^*}(r^*u_r^*)\right)\right] \tag{22}$$

$$\frac{\partial T^*}{\partial t^*} + \frac{1}{r^*}\frac{\partial}{\partial r^*}(r^*u_r^*T^*) + \frac{\partial}{\partial x^*}(u_x^*T^*) = \frac{2}{\text{Re}\cdot\text{Pr}}\left\{\frac{1}{r^*}\frac{\partial}{\partial r^*}\left(1 + C\text{RePr}\phi\frac{2R}{d_p}\left(\frac{\partial u_x^*}{\partial r^*}\right)\right)\left(r^*\frac{\partial T^*}{\partial r^*}\right) + \frac{\partial^2 T^*}{\partial x^{*2}}\right\} \tag{23}$$

Fig. 1 shows the geometrical configuration. It consists of the two dimensional laminar flow (r,x) of a nanofluid flowing inside a straight tube of circular cross-section geometry. It is enough to consider a half of the tube cross section due to the symmetric geometry.

To prevent non-physical pressure oscillations, staggered grids have been used. In the staggered grids, the velocity components are calculated at the center of the volume interfaces while the pressure as well as other scalar quantities such as fluid temperature is computed at the center of a control-volume [24].

The fluid enters the inlet section with uniform temperature (T_{in}) and uniform axial velocity profiles (u_{in}). The tube is long enough so that the fully developed flow conditions prevail at the outlet. On the tube wall, the usual non slip conditions are imposed; also, two different thermal boundary conditions have been considered in this study; namely, the uniform wall heat flux and the uniform wall temperature conditions. The flow and the thermal field are assumed to be symmetrical with respect to the vertical plane passing through the tube main axis. The boundary conditions and Nusselt number equation are rewritten using the dimensionless variables considering two different thermal boundary conditions.

To solve the equation set, projection method is applied. Projection method is a second order finite difference method. The general procedure for projection methods is a predictor-corrector approach. In a first step a preliminary velocity field $(\vec{v})$ is computed utilizing the momentum equations. By using this preliminary velocity, the momentum equation is divided into two parts as follows:

$$\frac{\vec{v} - \vec{u}^{*n}}{\Delta t^*} + \nabla\left(\vec{u}^{*n}\cdot\vec{u}^{*n}\right) = \frac{2}{\text{Re}}\nabla^2\vec{u}^{*n} \tag{24}$$

$$\frac{\vec{u}^{*n+1} - \vec{v}}{\Delta t^*} + \vec{\nabla}\, p^{*n+1} = 0 \tag{25}$$

It is evident that the preliminary velocity does not satisfy the continuity equation. In a second step a Poisson-type equation for the pressure is solved which is derived using the continuity equation and equation 25. In the last step the preliminary velocity field is projected onto a divergence-free velocity field using the computed pressure. Homogenous Neumann boundary condition for pressure and preliminary velocity is used [24].

The projection method is an appropriate option since the problem has a simple geometry and the method is a second order one.

The dispersion model has been successfully validated by applying this model to pure fluid flowing inside the tube; there is a good agreement between the obtained results from dispersion

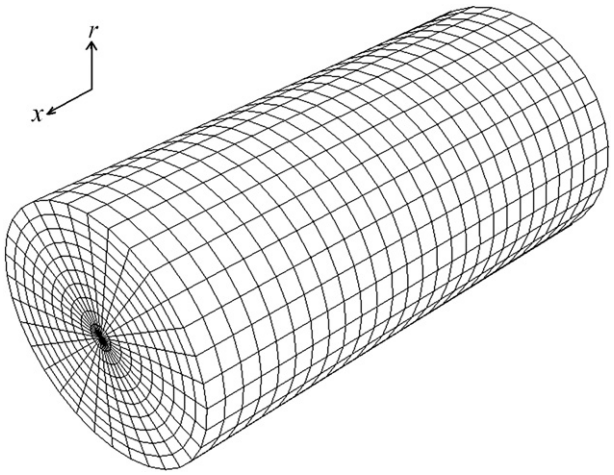

Fig. 1. Equal interval meshes in all directions.

Table 1
Comparison of the dispersion model and the homogenous model with the experimental results versus the Reynolds number for the water–Al_2O_3 nanofluid.

Re	$Nu_{q=cte}$			Error (%)	
	Experimental	Dispersion model	Homogenous model	Dispersion model	Homogenous model
725	5	5.83	4.93	16.53	−1.43
1060	6.7	6.71	5.34	0.11	−20.30
1320	7.5	7.39	5.63	−1.48	−24.90
1600	8.1	8.12	5.92	0.26	−26.86
1810	9	8.67	6.13	−3.65	−31.89

Table 2
Comparison of the dispersion model and the homogenous model with the experimental results versus the volume concentration for the water-Al_2O_3 nanofluid.

ϕ	$Nu_{q=cte}$			Error (%)	
	Experimental	Dispersion model	Homogenous model	Dispersion model	Homogenous model
0	5.3	5.43	5.43	2.38	2.38
0.6	6.6	6.24	5.38	−5.47	−18.52
1	6.7	6.71	5.34	0.11	−20.30
1.6	7.1	7.36	5.30	3.71	−25.40

model and the analytical and numerical data by others. The results of a pure fluid can be achieved by means of using the dispersion model for a nanofluid with zero nanoparticles volume fraction.

The equations (20)–(22) evidently are the same for nanofluid and pure fluid, in other words, the thermal dispersion model has no effect on the momentum equation. So the dimensionless velocity profile and friction factor for the nanofluid flowing in the tube are almost equal to those of pure fluid. Consequently the nanofluid flowing in the tube incurring either little or no penalty in pressure drop in comparison with the pure fluid. This is one of the important advantages of nanofluids compared with the suspended particles of millimeter or micrometer dimensions that is widely mentioned in literature [1,3,4,6,25]. This fact confirms the non-dependency of momentum equation from thermal dispersion model.

5. Nanofluid heat transfer

The dispersion model has been applied for various nanofluids using experimental thermal properties. In order to calibrate the model for a special nanofluid, a base point is selected between the reported experimental data. Some arbitrary values for the dispersion coefficient are selected to evaluate the Nusselt numbers using the developed model and calculated Nusselt numbers are plotted versus the selected dispersion coefficients. Then, using an interpolating procedure, the appropriate value for the nanofluid dispersion coefficient can be determined in such a way that the model can predict the same result for the base point compared to experimental result. The nanofluid dispersion coefficient can be determined based on any reported experimental data. Also an averaging method has been examined. In this method, the nanofluid dispersion coefficient was obtained for all of the reported experimental points and the average value of these coefficients proposed as proper nanofluid dispersion coefficient. Contrary to the expectation, this averaged nanofluid coefficient cannot predict the nanofluid behavior properly as well as using a proper single base point.

5.1. De-ionized water-γ-Al_2O_3 nanofluid

Wen and Ding have carried out an experimental work in 2004. The nanoparticles that they used in their work, was γ-Al_2O_3 with a size range of 27–56 nm, de-ionized water was used as the base liquid. The effective thermal conductivity of nanofluids was measured by using the transient hot wire method. Einstein equation was used to estimate the viscosity of the nanofluid. A straight copper tube with 970 mm length, 4.5 mm inner diameter, and 6.4 mm outer diameter was used as the test section. A constant heat flux condition along the test section has been provided and the results are presented in dimensionless length $x^* = 232$ [1]. The selected experimental data as the base point are Re = 1060, $\phi = 1\%$ and $x^* = 232$.

The reported Nusselt number at this point is Nu = 6.7 [1].

To verify the nanofluid model with the experimental results, the model should be calibrated in the base point. The calculated value for the dispersion coefficient that calibrates the model is $C = -1.458 \times 10^{-8}$.

Table 1 presents the obtained results of numerical modeling both the dispersion and homogenous models and the experimental results in which the Nusselt number versus the Reynolds number are reported. Fig. 2 shows these results clearly.

Almost relative agreement between the dispersion model and the experimental results is seen and the maximum discrepancy is 4% except for the first point; while the discrepancy of the homogenous model and the experimental results are between 20 and 31% over the same Reynolds number range.

The effect of volume concentration on Nusselt number is indicated in Table 2. These results are also indicated in Fig. 3.

It is clear from Fig. 3 that the maximum discrepancy of the dispersion model and the experimental results is 5%; while the

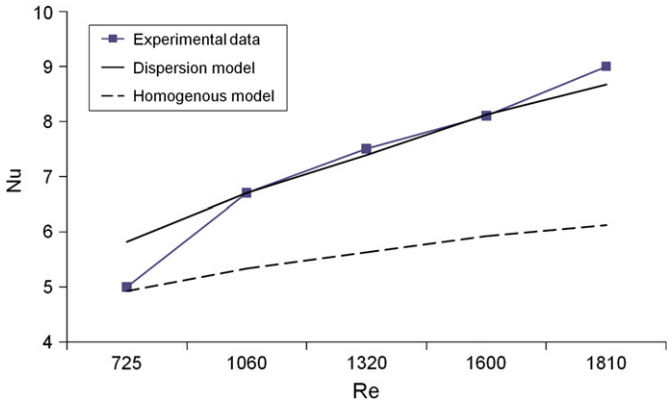

Fig. 2. Comparison of the dispersion model and the homogenous model with the experimental results versus the Reynolds number for the water–Al_2O_3 nanofluid.

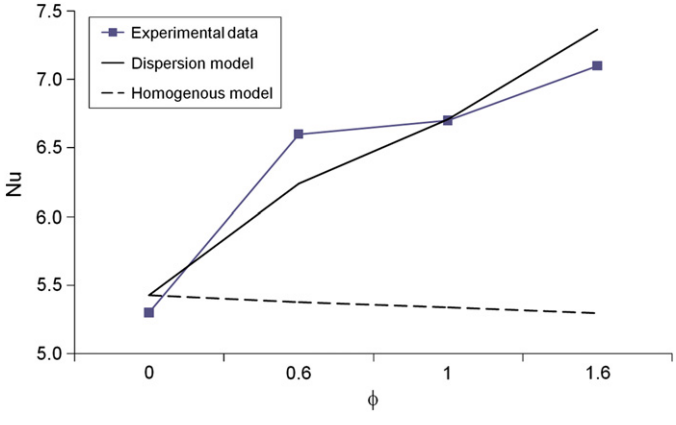

Fig. 3. Effect of volume concentration on Nusselt number for the dispersion and homogenous models and the experimental results for the water–Al_2O_3 nanofluid.

Table 3
Effect of Reynolds number on Nusselt number for the dispersion and homogenous models and the experimental results for the ATF–graphite nanofluid.

Re	$Nu_{q=cte}$			Error (%)	
	Experimental	Dispersion model	Homogenous model	Dispersion model	Homogenous model
19.47	6.30	5.85	5.40	−7.10	−14.25
25.43	6.92	6.63	5.97	−4.24	−13.76
31.75	7.55	7.39	6.49	−2.13	−14.09
38.07	8.07	8.09	6.92	0.20	−14.20
44.03	8.69	8.70	7.28	0.08	−16.22
50.35	8.69	9.32	7.62	7.19	−12.30
56.67	9.32	9.91	7.93	6.34	−14.88

discrepancy of the homogenous model and the experimental results is between 18 and 25% over the same volume fraction range.

It is worthy to mention that the experimental results have certainly a measurement inaccuracy. For measuring instrumentations, if a smooth curve is fitted into the experimental results, a full agreement could be seen and the discrepancy will decrease.

5.2. ATF–graphite nanofluid

This experiment was accomplished in 2005 by Yang et al. The nanoparticles used in this research were discus shape graphitic with the average diameter of about 1–2 μm, and the thickness around 20–40 nm. The base fluid was a commercial automatic transmission fluid (ATF). A smooth tube with 45.7 cm length, 0.457 cm inner diameter, and 0.635 cm outer diameter was used as the test section. The nanofluid properties were measured experimentally. The mixtures Prandtl number was above 500 and the flow Reynolds number was below 60. A constant heat flux condition along the test section was provided and the results were presented in dimensionless length of $x^* = 200$ [10].

The calculated value for the dispersion coefficient that calibrates the model is $C = -1.468 \times 10^{-9}$.

Table 3 and Fig. 4 show the effect of Reynolds number on the convective heat transfer coefficient.

It is obvious that the nanofluid model is in good agreement with the experimental results and the discrepancy is less than 7%; while the homogenous model discrepancy is nearly 14%. Table 4 and Fig. 5 show the nanoparticle volume concentration effect on the heat transfer coefficient.

Again, reasonably good agreement is seen except in the first point and the discrepancy is less than 0.7%; while the homogenous model discrepancy is nearly 19%. A measuring inaccuracy seems at the first point, because the volume concentration is zero. This means that the fluid is pure and its convective heat transfer could be predicted by the homogenous model.

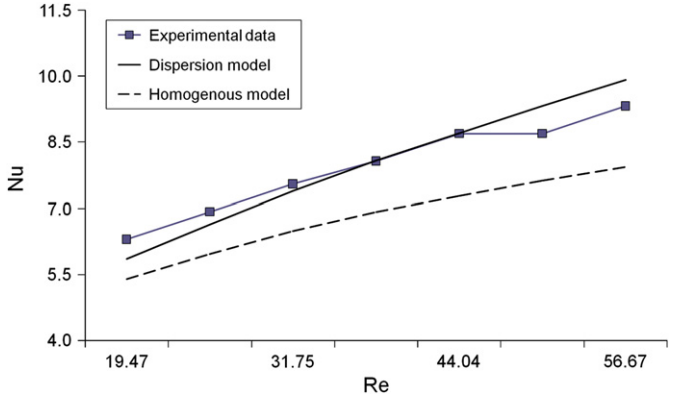

Fig. 4. Effect of Reynolds number on Nusselt number for the dispersion and homogenous models and the experimental results for the ATF–graphite nanofluid.

Table 4
Influence of volume concentration on Nusselt number for the dispersion and homogenous models and the experimental results for the ATF–graphite nanofluid.

ϕ	$Nu_{q=cte}$			Error (%)	
	Experimental	Dispersion model	Homogenous model	Dispersion model	Homogenous model
0	10.62	7.78	7.78	−26.78	−26.78
2	8.07	8.09	6.92	0.20	−14.21
2.5	8.80	8.74	7.12	−0.70	−19.03

5.3. Water–Al_2O_3 nanofluid

Zeinali et al. have carried out an experimental work in 2007. They used The Al_2O_3 nanoparticles with the size of about 20 nm in water as the base fluid. A smooth tube with 100 cm length, 0.6 cm inner diameter, and 0.7 cm outer diameter was used as the test section. The nanofluid properties are calculated using the classical formulas for two phase fluids (equations (1)–(4)). A constant temperature condition along the test section has been provided and the results are presented in dimensionless length of $x^* = 333.3$ [25].

The calculated value for the dispersion coefficient that calibrates the model is $C = -7.852 \times 10^{-9}$.

The effect of Reynolds number on Nusselt number is indicated in Table 5 and Fig. 6 respectively.

It is considered that the nanofluid model is in good agreement with the experimental results and the discrepancy is less than 3%.

6. Effect of nanoparticle size on nanofluid convective heat transfer

The relationship between the nanoparticle size and the nanofluid heat transfer coefficient has not been studied experimentally. This subject has been investigated using the dispersion model in this section. This study will be carried out using water-Al_2O_3 nanofluid with 1.0% volume concentration in Re = 1060. The effective conductivity for different nanoparticle size has been derived from Xue & Wen-mei Xu work [16] that is shown in Fig. 7.

The dispersion model has been used for the nanofluids with different nanoparticle size and the results have been presented in Fig. 8 for the constant heat flux condition.

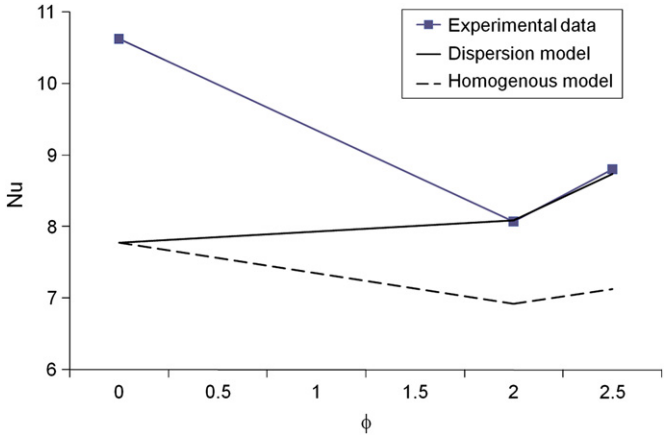

Fig. 5. Influence of volume concentration on Nusselt number for the dispersion and homogenous models and the experimental results for the ATF–graphite nanofluid.

Table 5
Comparison of the dispersion model and the experimental results versus the Reynolds number for the water-Al_2O_3 nanofluid.

Re	$\overline{Nu}_T$ = cte		Error (%)
	Experimental	Dispersion model	
391.7	5.02	5.18	3.13
491.6	5.51	5.57	0.98
543.0	5.78	5.76	−0.27
691.6	6.36	6.34	−0.39
791.5	6.71	6.73	0.34
880.7	7.02	7.08	0.77
988.7	7.32	7.50	2.51

Zeinali et al. work is one of the experimental results for water-Al_2O_3 nanofluid. This experimental study is based on a nanofluid with 20 nm Al_2O_3 nanoparticles but Re = 1060 is not reported by this experiment and a constant wall temperature is provided as the boundary condition. Considering the good agreement between the experimental results that reported in this research and the dispersion model predictions for various Reynolds numbers (above mentioned in Fig. 6 and Table 5), the calibrated dispersion model is used for this special case. In such a way the obtained result for the heat transfer coefficient was 7.45. The discrepancy of this value and the results plotted in Fig. 8 is nearly 8.81% that shows a reasonably acceptable agreement (Fig. 9).

An inspection of Figs. 7 and 8 also indicates that the dependence of the thermal conductivity and the heat transfer coefficient on the nanoparticle size is negligible for the suspensions that contain large particles of the order of micrometers. These results were expected according to the conventional correlations for the suspensions thermal conductivity and Nusselt number and confirm the dispersion model results for the dependence of heat transfer to the nanoparticle size. Thermal conductivity of the solid-liquid mixtures with particles of the order of micrometers or millimeters can be calculated using theoretical models like Hamilton and Crosser model (equation (4)) [12]. Heat transfer coefficient of these suspensions will be calculated applying the homogenous model that is to use the correlations for the conventional fluids with the suspension effective properties.

Fig. 10 plots the dependence of thermal conductivity on nanoparticle size again (Fig. 7); also shown in the figure is predictions by the Hamilton and Crosser model. Fig. 11 shows the dependence of Nusselt number on nanoparticle size again (Fig. 8); also shown in the figure is predictions by the homogenous model.

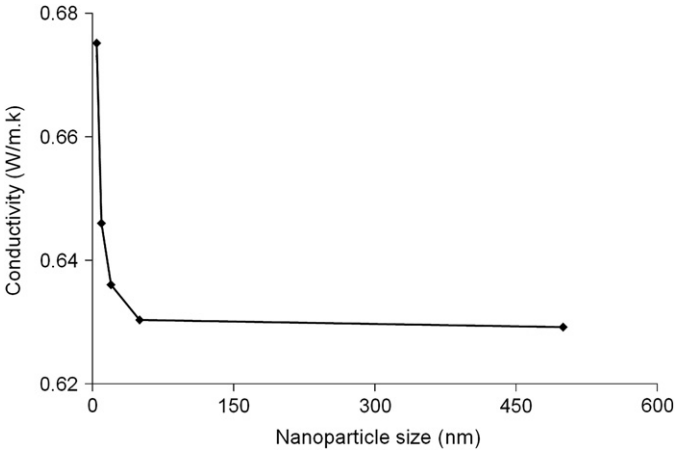

Fig. 7. Dependence of nanoparticle size on the effective thermal conductivity for water–Al_2O_3 nanofluid according to Xue & Wen-mei Xu research [13].

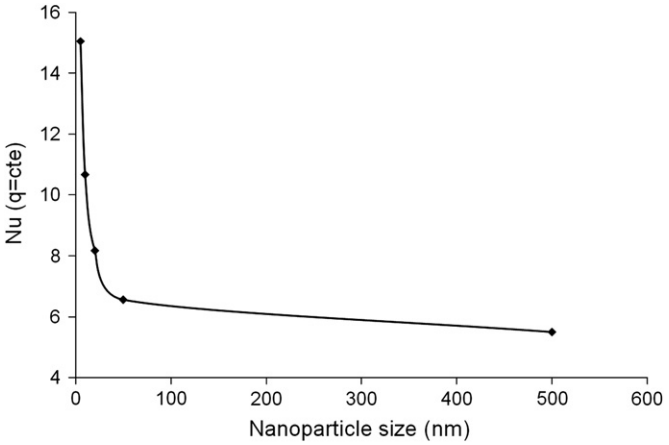

Fig. 8. Variation of Nusselt number versus the nanoparticle size for water–Al_2O_3 nanofluid based on the dispersion model.

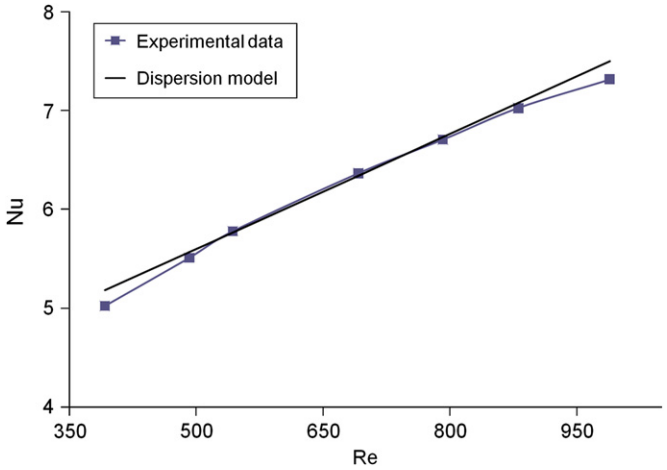

Fig. 6. Effect of Reynolds number on Nusselt number for the dispersion model and the experimental results the water–Al_2O_3 nanofluid.

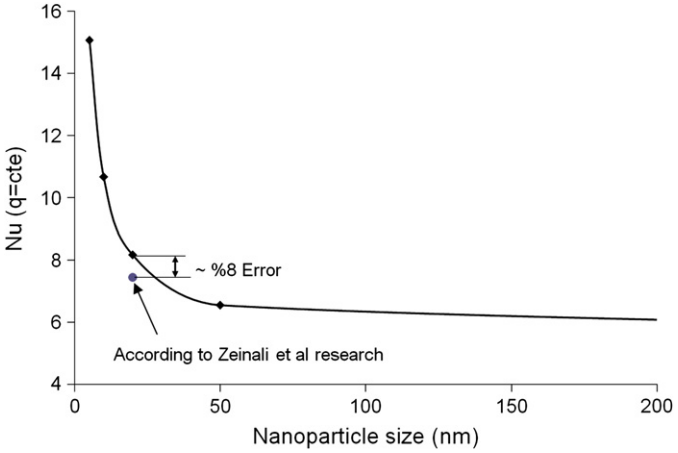

Fig. 9. Good agreement between the result predicted by dispersion model for a nanofluid with 20 nm nanoparticles and the experimental result by Zeinali et al.

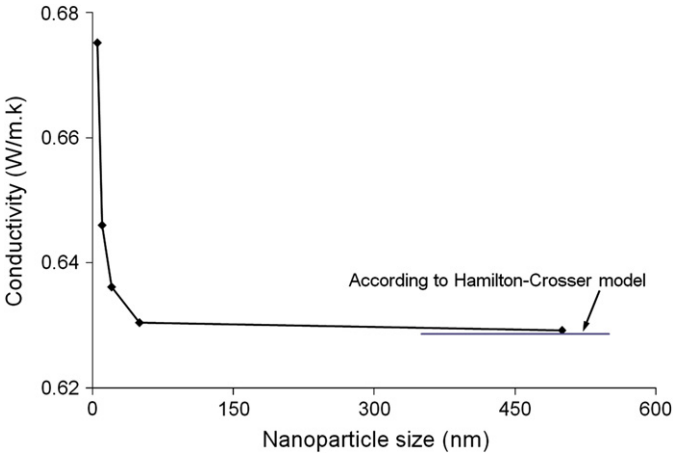

Fig. 10. Dependence of thermal conductivity on nanoparticle size predicted by Xue & Wen-mei Xu research (Fig. 7) and the Hamilton and Crosser model.

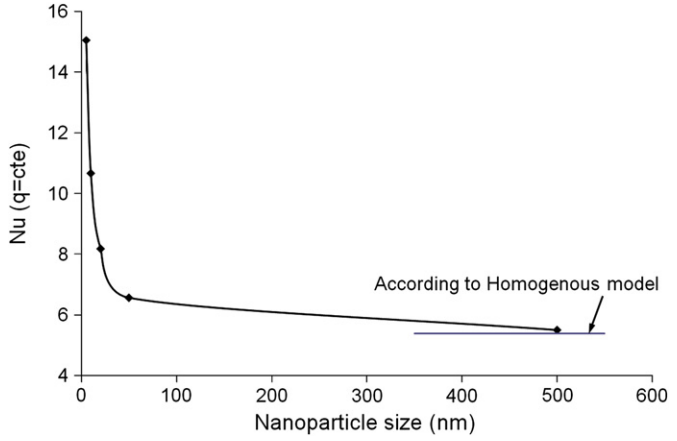

Fig. 11. Dependence of Nusselt number on nanoparticle size according to the dispersion model (Fig. 8) and the homogenous model.

It is clear from Figs. 10 and 11 that the curves of nanofluid thermal conductivity and heat transfer coefficient tend to a constant value which predicted by Hamilton & Crosser model and homogenous model respectively for the particles larger than 500 nm (0.5micron) and the dependence of the thermal conductivity and Nusselt number on the nanoparticle size becomes negligible.

7. Conclusion

1. The dispersion model was used to investigate the laminar convective heat transfer of nanofluids through a tube. Mathematical expression of the dispersion phenomena in porous media had been published. In this work, a correlation was used for the dispersion in the nanofluid subject. The results obtained from the dispersion model were compared with the existing experimental results for three kinds of nanofluids. Comparisons indicate good agreement between the dispersion model and the experimental results. In regard to volume fraction variations, the discrepancy is less than 2.5% and rarely exceeds 5% and for the variations of Reynolds number the discrepancy is less than 4% and rarely goes beyond 7%. While the homogenous model predictions generally show a discrepancy in the range of 14–30%. So the dispersion model predicts the nanofluid heat transfer behavior reliably.
2. The conventional correlations for the suspensions heat transfer coefficient are not dependant on the particle size and only depend on the particle volume fraction. In this work, it is shown that these correlations are not valid for the suspensions that contain particles smaller than 0.5 micron (500 nm) and the less particle size, the dramatically more heat transfer coefficient. The dispersion model can predict the dependence of nanofluid heat transfer coefficient on nanoparticle size properly.

References

[1] D. Wen, Y. Ding, Experimental investigation into convective heat transfer of nanofluids at the entrance region under laminar flow conditions. Int. J. Heat Mass Trans. 47 (2004) 5181–5188.
[2] U.S. Choi, Enhancing thermal conductivity of fluids with nanoparticles. ASME FED 231 (1995) 99–103.
[3] Y. Xuan, W. Roetzel, Conceptions for heat transfer correlation of nanofluids. Int. J. Heat Mass Trans. 43 (2000) 3701–3707.
[4] Y. Xuan, Q. Li, Investigation on convective heat transfer and flow features of nanofluids. J. Heat Trans. ASME 125 (2003) 151–155.
[5] V. Trisaksri, S. Wongwises, Critical review of heat transfer characteristics of nanofluids. Renew. Sust. Energ. Rev. 11 (3) (2007) 512–523.
[6] Y. Xuan, Q. Li, Heat transfer enhancement of nanofluids. Int. J. Heat Fluid Fl 21 (2000) 58–64.
[7] Y. Sato, E. Deutsch, O. Simonin, Direct numerical simulations of heat transfer by solid particles suspended in homogeneous isotropic turbulence. Int. J. Heat Fluid Fl 19 (2) (1998) 187–192.
[8] A. Behzadmehr, M. Saffar-Avval, N. Galanis, Prediction of turbulent forced convection of a nanofluid in a tube with uniform heat flux using a two phase approach. Int. J. Heat Fluid Fl 28 (2) (2007) 211–219.
[9] S. Maiga, S.J. Palm, C.T. Nguyen, G. Roy, N. Galanis, Heat transfer enhancement by using nanofluids in forced convection flows. Int. J. Heat Fluid Fl 26 (2005) 530–546.
[10] Y. Yang, Z.G. Zhang, E.A. Grulke, W.B. Anderson, G. Wu, Heat transfer properties of nanoparticle-in-fluid dispersions (nanofluids) in laminar flow. Int. J. Heat Mass Trans. 48 (6) (2005) 1107–1116.
[11] D.A. Drew, S.L. Passman, Theory of Multicomponent Fluids. Springer, Berlin, 1999.
[12] R.L. Hamilton, O.K. Crosser, Thermal conductivity of heterogeneous two-component systems. Ind. Eng. Chem. Fund 1 (1962) 182–191.
[13] P. Keblinski, S.R. Phillpot, S.U.S. Choi, J.A. Eastman, Mechanisms of heat flow in suspensions of nano-sized particles(nanofluids). Int. J. Heat Mass Trans. 45 (2002) 855–863.
[14] J.A. Eastman, S.U.S. Choi, S. Li, W. Yu, L.J. Thomson, Anomalously increased effective thermal conductivities of ethylene glycol-based nanofluids containing copper nanoparticles. Appl. Phys. Lett. 78 (2001) 718–720.
[15] J. Koo, C. Kleinstreuer, Impact analysis of nanoparticle motion mechanisms on the thermal conductivity of nanofluids. Int. Commun. Heat Mass 32 (2005) 1111–1118.
[16] Q. Xue, Wen-Mei Xu, A model of thermal conductivity of nanofluids with interfacial shells. Mater. Chem. Phys. 90 (2005) 298–301.
[17] H. Xie, M. Fujii, X. Zhang, Effect of interfacial nanolayer on the effective thermal conductivity of nanoparticle–fluid mixture. Int. J. Heat Mass Trans. 48 (2005) 2926–2932.
[18] L. Xue, P. Keblinski, S.R. Phillpot, S.U.-S. Choi, J.A. Eastman, Effect of liquid layering at the liquid–solid interface on thermal transport. Int. J. Heat Mass Trans. 47 (2004) 4277–4284.
[19] Q.Z. Xue, Model for effective thermal conductivity of nanofluids. Phys. Let. A 307 (2003) 313–317.
[20] Y. Ding, D. Wen, Particle migration in a flow of nanoparticle suspensions. Powder Technol. 149 (2005) 84–92.
[21] J. Bear, Dynamics of Fluids in Porous Media Second printing. American Elsevier Publishing Company, 1975.
[22] M. Kaviany, Principles of Heat Transfer in Porous Media. Springer Publication, New York, 1995.
[23] T. Baron, Generalized graphic method for the design of fixed end catalytic reactor. Chem. Eng. Prog. 48 (1952) 118–124.
[24] J.D. Anderson, Computational Fluid Dynamics: the Basics with Applications. McGraw Hill, New York, 1995.
[25] S.H. Zeinali, M. Nasr Esfahany, S.Gh. Etemad, Experimental investigation of convective heat transfer of Al_2O_3/water nanofluid in circular tube. Int. J. Heat Fluid Fl 28 (2) (2007) 203–210.